Targeted knock-down of a structurally atypical zebrafish 12S-lipoxygenase leads to severe impairment of embryonic development

Ulrike Haas[a,1], Elisabeth Raschperger[b,1], Mats Hamberg[a], Bengt Samuelsson[a], Karl Tryggvason[b], and Jesper Z. Haeggström[a,2]

[a]Division of Chemistry 2; and [b]Division of Matrix Biology, Department of Medical Biochemistry and Biophysics, Karolinska Institutet, S-171 77 Stockholm, Sweden

Contributed by Bengt Samuelsson, October 18, 2011 (sent for review September 19, 2011)

Lipoxygenases (LO) are a class of dioxygenases, which form hydroperoxy, hydroxy, and epoxy derivatives of arachidonic acid with distinct positional and stereochemical configurations. In man, there are two known types of 12-LO that are distinguished by their expression patterns and catalytic properties. The platelet 12S-LO plays a role in platelet aggregation and 12R-LO seems to be important for normal skin function. Using BLAST searches of the zebrafish (zf) genome we identified one candidate zf12-LO gene with 43% identity with human 12R-LO at the mRNA level and the deduced primary sequence carried the so called "Coffa" structural determinant (Gly residue) for R stereoselectivity of LOs. However, incubations of recombinant, purified, zf12-LO with arachidonic acid revealed exclusive formation of 12(*S*)-hydroperoxy-eicosatetraenoic acid. Further studies with immunohistochemistry showed prominent expression of zf12-LO in the cell nuclei of skin epithelium, the epithelial lining of the stomodeum, and the pharyngeal pouches in zf embryos. To probe its function, zf12-LO was subjected to targeted knock-down in zf embryos, resulting in the development of a severe phenotype, characterized by abnormal development of the brain, the eyes, and the tail as well as pericardial and yolk sac edema. Hence, we have identified a unique vertebrate 12S-LO that breaks the current structure-function paradigms for S and R stereo-specificity and with critical roles in normal embryonic development.

12-lipoxygenase | stereospecificity

Lipoxygenases (LO) are a class of nonheme iron containing dioxygenases, which incorporate molecular oxygen into polyunsaturated fatty acids like arachidonic and linoleic acid (1). The resulting hydroperoxy derivatives are implicated in cell maturation, atherogenesis, and cancer and are further metabolized to leukotrienes and lipoxins (2–5). The mammalian LO enzyme family consists of three major groups, 5-, 12-, and 15-LO, where the number indicates their positional specificity for insertion of oxygen into arachidonic acid.

The oxygenation reaction occurs with a high degree of stereospecificity, leading to either S or R chirality in the product. The structure of the active center is conserved among LOs with three canonical His residues and a C-terminal Ile binding the catalytic nonheme iron (6). The stereospecificity appears to depend on the architecture of the substrate binding pocket, which in turn determines the head-to-tail orientation and depth of the substrate penetration into the active site (6). Recent work describes the importance of a conserved amino acid at the active site for the S and R specificity of LOs (7). Thus, the so called "Coffa site" is defined by a conserved Ala in S-specific LOs whereas R-selective LOs carry a Gly residue at this position (Fig. S1). The only known exception to this rule among vertebrate S-LOs is the mouse platelet-type 12S-LO, which has a Ser instead of a Ala at this position (7).

Only two 12-LO isoforms are expressed in man; i.e., platelet-type 12S-LO and 12R-LO (8, 9). In mammals, the S-type 12-LOs are implicated in cell death and oxidative stress, carcinogenesis, and inflammatory processes of the cardiovascular system (2, 10, 11). The 12R-LO participates in proliferative processes of the skin such as wound healing and certain skin diseases, particularly those linked to permeability barrier insufficiencies (8, 12). Knock-out studies in mice showed no significant changes in the development of 12S-LO −/− embryos and only mild phenotypic alterations (13), whereas the knock-out of 12R-LO was associated with severe dysfunction of the skin barrier (14).

Danio rerio (zebrafish) has emerged as an excellent model for the study of early vertebrate development. The zebrafish (zf) embryos allow studies of gene function in the absence of maternal compensation and their optical clarity permits real-time visualization of organogenesis. Gene functions can be studied by targeted knock-down using Morpholino-modified antisense Oligonucleotides (MOs) and many mutations in zf lead to phenotypes resembling human diseases (15, 16). Here we report the identification of a zf12-LO, which carries the Coffa determinant of an R-lipoxygenase in its primary structure and yet displays a highly selective S-stereospecificity. Notably, knock-down of this enzyme reveals an important role in normal embryonic development and identifies a vertebrate S-lipoxygenase which is indispensible for life.

Results

Identification of a Zebrafish 12-LO Candidate. After BLAST searching of the zf whole genome shotgun assembly Zv7 (Sanger Institute), the 12-LO cDNA (*alox12*) was found to correspond to a gene region on chromosome 7. This gene has 16 exons spanning over 3.5 kb of genomic DNA. The ORF consists of 2,010 nucleotides (RefSeq accession number NM_199618) and the predicted protein contains 670 amino acids with ∼43% overall amino acid identity to other mammalian 12-LOs. Table S1 summarizes the sequence identity of the zf enzyme with other mammalian and amphibian LOs. The three iron binding His residues (hp12S-LO: His367, His372, and His547) as well as the carboxy-terminal Ile, which is also essential for the iron binding, are found in the zf protein (Fig. S2). Regarding the amino acids responsible for the oxygenation stereospecificity in LOs, the zf enzyme exhibits a Glu at position 358 and, more importantly, a Gly at position 410, indicating a 12R-LO activity of the enzyme (Fig. S1).

Author contributions: U.H., E.R., M.H., B.S., K.T., and J.Z.H. designed research; U.H., E.R., and M.H. performed research; U.H., E.R., M.H., and J.Z.H. analyzed data; and U.H. and J.Z.H. wrote the paper.

The authors declare no conflict of interest.

Freely available online through the PNAS open access option.

[1]U.H. and E.R. contributed equally to this work.

[2]To whom correspondence may be addressed. E-mail: jesper.haeggstrom@ki.se or bengt.samuelsson@ki.se.

This article contains supporting information online at www.pnas.org/lookup/suppl/doi:10.1073/pnas.1117094108/-/DCSupplemental.

Cloning, Expression, and Characterization of zf12-LO. To analyze the product profile of zf12-LO, the cDNA was amplified and cloned into the vector pPICZ A followed by expression of the enzyme in *Pichia pastoris* and purification to apparent homogeneity. The final yield was 1–2 mg protein/L yeast culture and the purity at least 95% as judged from SDS-PAGE (Fig. S3). Incubation of the recombinant enzyme with arachidonic acid followed by borohydride reduction led to a single major product, *viz.*, 12-hydroxyeicosatetraenoic acid (HETE), and small amounts of 8-HETE. From liquid chromatography-mass spectrometry analysis, the ratio of 12-HETE/8-HETE was calculated to 13.5/1 (Fig. 1*A*). To test if the protein follows the Coffa rule and produces 12(*R*)-HETE, the enzyme was incubated with arachidonic acid and the reaction products were analyzed by RP-HPLC (Fig. S4). The HPLC fractions containing 12-HETE and 8-HETE were collected and metabolites were methyl-esterified and analyzed by chiral-phase (CP) HPLC. When compared to standards of 12(*S*)-HETE methyl ester and 12(*R*)-HETE methyl ester, which eluted at 22.1 and 23.4 min, respectively, 12-HETE methyl ester derived from zf12-LO eluted with the same retention as the S-enantiomer (Fig. 1 *B* and *C*). Similarly, when 8-HETE methyl ester derived from zf12-LO was compared with synthetic standards of 8(*S*)-HETE methyl ester and 8(*R*)-HETE methyl ester (retention times 24.5 and 30 min), the enzyme derived product was found to be the R-enantiomer (Fig. 1 *D* and *E*). The enantiomeric purity was 94% or higher.

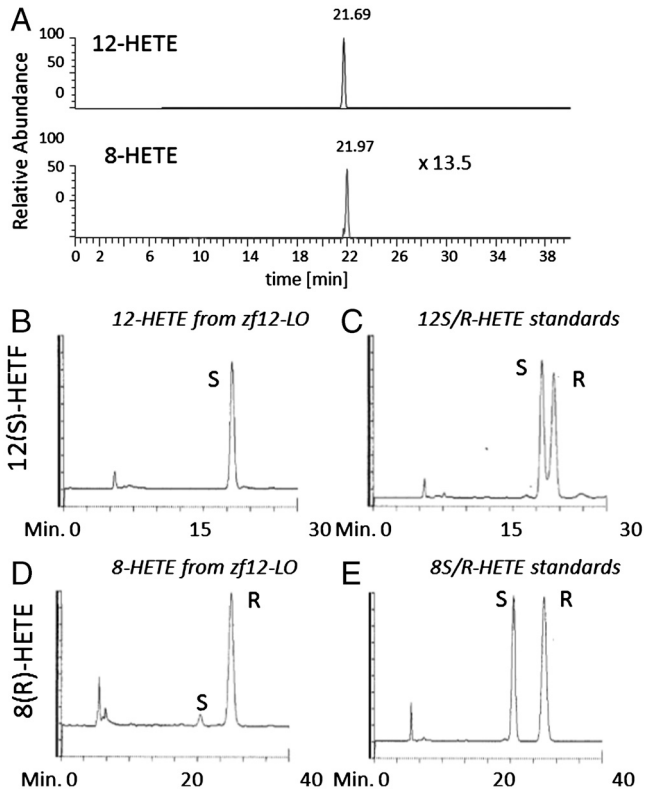

Fig. 1. LC-MS and CP-HPLC analyses of the products formed by recombinant zf12-LO. (*A*) For LC-MS analysis, recombinant enzyme was incubated with arachidonic acid and resulting compounds were analyzed by LC-MS. (*B*) CP-HPLC analysis of biologically derived 12-HETE-methyl ester (Me) resulted from zf12-LO. (*C*) CP-HPLC analysis of 12(*S*)-HETE-Me and 12(*R*)-HETE-Me standards. (*D*) CP-HPLC analysis of biologically derived 8-HETE-Me resulted from zf12-LO. (*E*) CP-HPLC analysis of 8(*S*)-HETE-Me and 8(*R*)-HETE-Me standards. CP-HPLC analyses were performed by using an OB-H column. Products were eluted with 2-propanol-hexane (2:98, vol/vol) at a flow rate of 0.5 mL/ min and absorbance at 234 nm.

Expression Pattern of zf12-LO in Early Zebrafish Development. Transversal cryosections of zf embryos at two days post fertilization (dpf) were stained for zf12-LO, using a rabbit anti-zf12-LO polyclonal antiserum. Nuclear expression of the protein was detected in the skin epithelium (Fig. 2 *A–C*) and in the epithelial lining of the stomodeum (Fig. 2*A*) and the pharyngeal pouches (Fig. 2*B*). The protein was not detected in the gut/kidney area of the embryos.

Knock-Down of zf12-LO Expression by Morpholino Oligonucleotides. To investigate the consequences of the knock-down of zf12-LO protein, two independent MOs were chosen as depicted in Fig. 3*A*. MO-1 was designed to block the translation of the protein, while MO-2 targeted the second exon-intron junction and led to an incorrect splicing of the mRNA. The effects of the MOs on gene expression were checked with RT-PCR analysis and measurement of enzyme activity, as assessed by 12-HETE formation (Figs. S5, S6). Changes in the phenotype, in comparison to untreated embryos (WT), were studied one and two dpf. Macroscopical analyses exposed dramatic and consistent changes in development of MO-1 morphants already at one dpf (Fig. 3 *B–D*). The head was less developed and the tail was bent (Fig. 3*C*) compared to control embryos (Fig. 3 *B* and *D*). A similar phenotype was seen for MO-2 morphants. This phenotype became more pronounced at two dpf (Fig. 3 *E–I*) and was seen in 93% of scored MO-1 morphants (Table 1). Embryos treated with MO-1 displayed a severe phenotype (86%) with bending and spiraling of the tail, pericardial and yolk sac edema and a delayed development of the head (Fig. 3*F*). Additionally, a decreased blood flow as well as a slower heart beat was observed. The morphants also showed minimized movements compared to WT and MO-1 mis treated embryos. The same was observed when embryos were treated with MO-2 (Fig. 3*H*) even if the phenotype was more heterogenous (Table 1). Thus, 78% of the MO-2 morphants demonstrated impaired development and the appearance of edemas and 35% were scored as severe. In contrast, WT embryos (Fig. 3 *B* and *E*) as well as embryos treated with corresponding

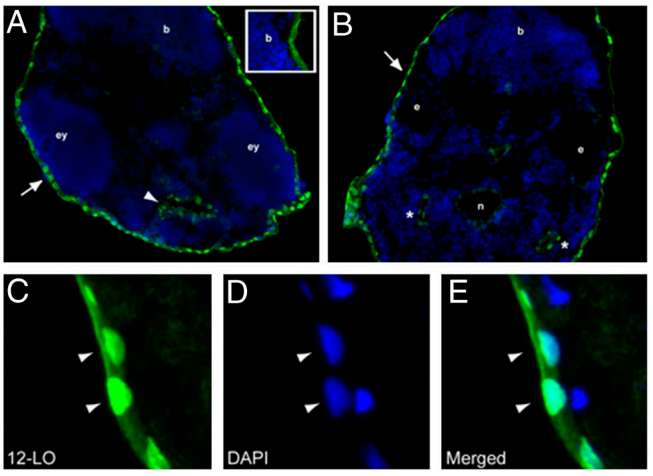

Fig. 2. Expression pattern of zf12-LO protein in zf embryos: Immunohistochemical staining of zf12-LO was performed on transversal sections from a two dpf embryo. Nuclear expression of zf12-LO was detected in the skin epithelium that surrounds the embryo (*A* and *B*, arrows) as well as the yolk sac. zf12-LO was also detected in the epithelial lining of the stomodeum (*A*, arrowhead) and the pharyngeal pouches (*B*, asterisks). Unspecific staining of the zf12-LO antibody is shown in insert in *A* and in the notochord (*B*). The notochord (*n*), brain (*b*), eyes (*ey*), and ear (*e*) are indicated for orientation. Epithelial cells at higher magnification (*C–E*) show nuclear localization of zf12-LO as assessed by colocalization (arrow heads) of zf12-LO immunostaining and DAPI staining (blue).

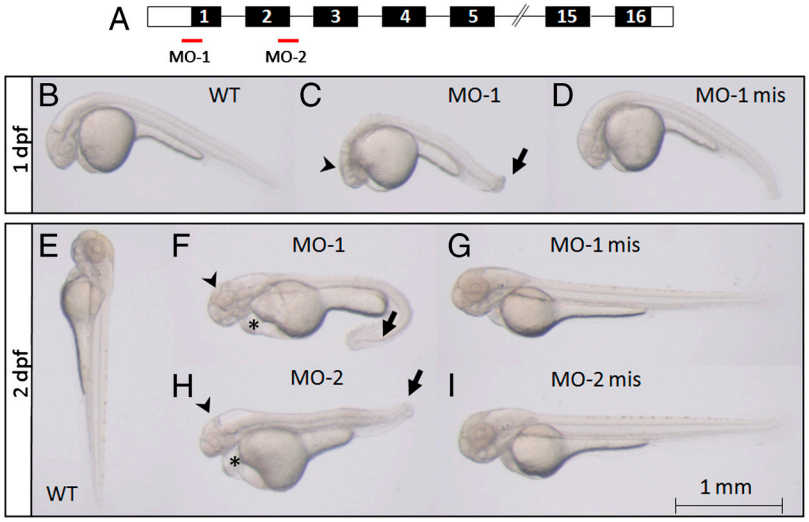

Fig. 3. Knock-down of zf12-LO leads to abnormal development of the head and tail as well as yolk sac and pericardial edema. (*A*) Two MOs, one complementary to the region of the ATG site blocking translation (MO-1) and another corresponding to the end of exon-2/ start of intron-2/3 blocking the correct splicing of exon-2 (MO-2) were designed. The exons of the zf12-LO gene, encoding the zf12-LO protein, are shown in black boxes and the 5′UTR and 3′UTR regions are marked with white boxes (not drawn to scale). Embryos were visualized by regular light microscopy at one dpf (*B–D*) and two dpf (*E–I*). Wild type (B) as well as MO-1 mis treated embryos (*D*) developed normally whereas injection of MO-1 (*C*) resulted in retarded development of the head (arrowhead) and a bent tail (arrow) already after one dpf. The phenotype was more pronounced in MO-1 morphants at two dpf (*F*). The head was less developed (arrowhead), the tail was strongly bent (arrow) and pericardial edema as well as edema around the yolk sac appeared (asterisk). A similar phenotype was observed in MO-2 treated embryos at two dpf (H). In contrast, WT (*E*) as well as embryos treated with MO-1 mis and MO-2 mis (*G* and *I*) developed normally. Animals shown are representative embryos for the indicated time points.

amounts of MO-1 mis (Fig. 3 *D* and *G*) or MO-2 mis (Fig. 3*I*) did not show any phenotypic alterations.

Microscopic Analysis of Transversal Sections of Morphants and Control Embryos. To further explore the morphological defects observed in embryos injected with MOs, Hematoxylin/Eosin-stained sections of morphants as well as control embryos (WT, MO-1 mis) at two dpf were compared. Transversal sections through the brain/eye layer of MO-1 morphants (Fig. 4*A*) revealed a clearly defect brain development when compared to MO-1 mis morphants (Fig. 4*D*). The size of the Mesencephalon as well as the Diencephalon was decreased compared to controls. A delayed development of the Myelencephalon was also observed in sections of the ear/heart region in MO-1 morphants compared to controls (Fig. 4 *B* and *E*). Additionally, a less structured basal plate was detectable in MO-1 morphants (Fig. 4*B*). Finally, an unstructured composition of the somites as well as severe edema around the yolk sac were observed in MO-1 treated embryos (Fig. 4*C*) but not in MO-1 mis morphants (Fig. 4*F*). In contrast, sections of MO-1 mis treated embryos (Fig. 4 *D–F*) showed no differences in the organ structures compared to sections of WT embryos.

Knock-down of zf12-LO with MO-1 or MO-2 also led to serious abnormalities in the eye development. The eyes of morphant embryos were smaller as compared to controls. Thus, the diameters of MO-2 morphant eyes, measured along two perpendicular axes, were shorter than the corresponding measures of eyes in WT embryos ($p < 0.0005$, $n = 5–10$). Similar results were obtained with MO-1 morphants. Of note, the distinct structured layers of the retina were absent in morphant embryos and the lens failed to develop crystalline content (Fig. 5).

Table 1. Total amount of embryos and percentage distribution of phenotypes in embryos treated with MOs at two dpf. WT: wildtype, mis: mispair, MO: antisense Morpholino oligonucleotide

Phenotype embryos	Normal	Moderate	Severe	*n*
WT	**98%**	2%	-	355
MO-1	7%	7%	**86%**	415
MO-1 mis	**91%**	8%	1%	388
MO-2	22%	**43%**	**35%**	340
MO-2 mis	**84%**	14%	2%	346

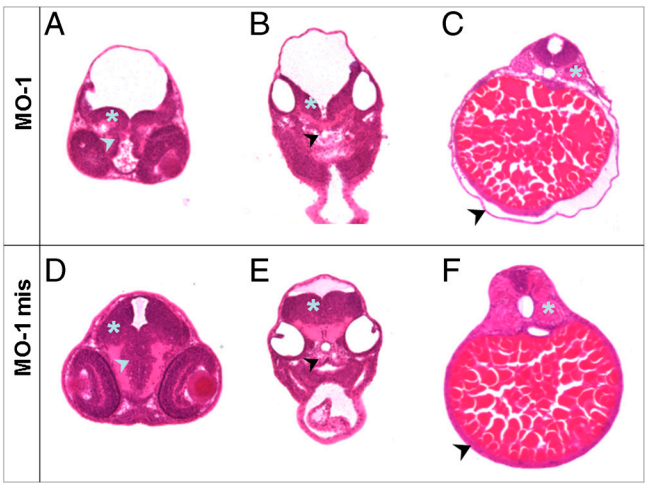

Fig. 4. Transversal sections through different layers of embryos at two dpf treated with MO-1 and MO-1 mis. Embryos were embedded in plastic, 10 μm transversal sections were prepared and counterstained with Hematoxylin/Eosin. The regions of eye/brain (*A* and *D*), ear/heart (*B* and *E*) and kidney/gut (*C* and *F*) were analyzed. (*A*) MO-1 treated embryos display a delayed development of the Mesencephalon (asterisk) as well as Diencephalon (arrowhead) compared to MO-1 mis treated embryos (*D*). (*B*) The decelerated development of the brain was also detectable in the Myelencephalon region (asterisk) in MO-1 morphants combined with an unstructured composition of the basal plate (arrowhead). (*E*) MO-1 mis treated embryos showed a normally developed Myelencephalon and a well constructed basal plate. (*C*) In the area of the kidney/gut, an edema located around the yolk sac was observed in MO-1 morphants (arrowhead). Furthermore, an unstructured composition of the somites was visible (asterisk). (*F*) These alterations were not observed in MO-1 mis treated embryos. Sections shown are from representative embryos for the indicated time points.

BIOCHEMISTRY

Discussion

Ever since the first discovery of a human 12-LO in platelets, this family of enzymes has attracted considerable attention and has been implicated in human diseases, particularly cancer and various dermatoses (11, 12). The number of 12-LOs varies among species and each isoform is classified according to its expression pattern, regio-, and stereospecificity. For instance, in mice four isoforms are known, namely platelet-type 12S-LO, leukocyte-type 12S-LO, epidermal-type 12S-LO, and 12R-LO (5), whereas in man only two 12-LOs are expressed; i.e., the platelet-type 12-LO, which is a strict S-lipoxygenase and 12R-LO with the opposite stereospecificity.

The zf12-LO has Structural Characteristics of an R-lipoxygenase but Displays a Strict S Stereospecificity. Lipoxygenases catalyze a dioxygenation of a 1,4-cis-pentadiene moiety in polyunsaturated fatty acids, typically arachidonic acid. The reaction proceeds according to a radical mechanism involving a catalytic, nonheme, iron that is bound by three canonical histidines as well as the C-terminal Ile (5). Regio- and stereoselectivity is thought to be governed by substrate binding and positioning, which in turn depends on the depth and architecture of the substrate binding pocket (7).

Aligning the zf12-LO amino acid sequence with other S and R-LOs reveals the presence of signatures comparable with those of a 12S-LO (Fig. S2). For instance, the zf12-LO carries a valine at position 425, corresponding to the Sloane determinant Val418 for positional specificity of 12S- rather than 15S-lipoxygenation (17). Mutation of Met418 into a Val in human 15-LO resulted in an enzyme which also displayed 12-LO activity. At one site, the so called Coffa site, an Ala predicts an S-lipoxygenase whereas a Gly is typical of an R-specific LO (7). Here, the zf12-LO carries a Gly indicating that it is an R-lipoxygenase. However, CP-HPLC analysis of 12-HETE formed by zf12-LO revealed an exclusive 12S-lipoxygenation of arachidonic acid (Fig. 1). Hence, zf12-LO represents an exception to the Coffa rule for structural determinants of S and R- stereospecificity of vertebrate LOs. This result in turn demonstrates that structures within zf12-LO, other than the Coffa site, govern the S stereospecificity, perhaps the above mentioned Sloan determinant which is not present in human and mouse 12R-LO (Fig. S2).

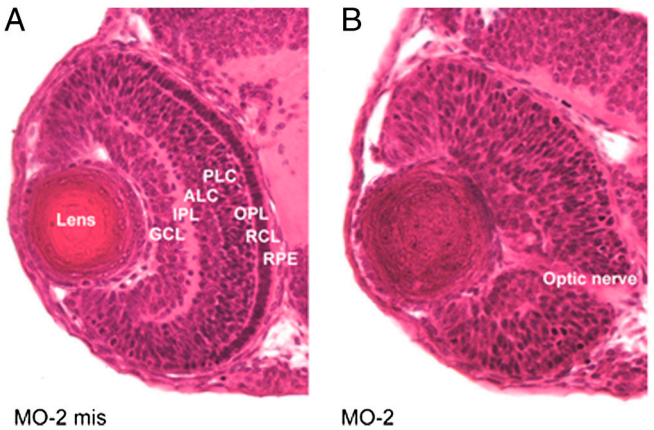

Fig. 5. Zf12-LO is required for normal eye development. Sections of zf embryos were prepared and stained with Hematoxylin/Eosin. Morphological comparison of zf12-LO morphants (treated with MO-2) and controls (treated with MO-2 mis) was carried out with light microscopy at two dpf. Injection of MO-2 results in developmental eye abnormalities including loss of retinal layered structures and lens crystalline. RPE; retinal pigmented epithelium, RCL; rods and cones layer, OPL; outer plexiform layer, BCL; bipolar cell layer, ACL; amacrine cell layer, IPL; inner plexiform layer, GCL; ganglion cell layer. Similar results were obtained with zf12-LO morphants treated with MO-1.

Knock-Down of zf12-LO Leads to a Severe Phenotype. Contrary to what would be expected for an S-lipoxygenase, knock-down of zf12-LO resulted in severe impairment of embryonic development, a lethal phenotype demonstrating that zf12-LO is indispensible for life. Thus, serious abnormalities were observed in the development of the brain, eyes, and tail, along with pericardial and yolk sac edema (Figs. 3–5). Within the brain, the Mesencephalon as well as the Myelencephalon consisted of fewer cell layers and the Diencephalon was underdeveloped, as emphasized by a smaller cell mass. In addition, eyes of morphant embryos were smaller than those of control embryos and had almost completely lost the layered structures of the retina, typical of normal embryonic development (Fig. 5).

Previous studies have implicated 12-LO and 12-LO metabolites in brain function. For instance, a 12-LO activity in *Aplysia Californica* has been suggested to play a role in neuronal signaling and earlier studies in rats showed that 12-LO is the most commonly expressed LO in the brain localized to cortical neurons, astrocytes as well as in oligodendrocytes (18). Possibly, 12-LO metabolites act as second messengers and participate in cell-cell communication and may also interact with nuclear factors producing physiological responses and morphological changes when generated during cell development (19). Hence, one may speculate that zf12-LO is involved in regulating the growth and function of the fish brain, possibly reflecting similar roles in mammals.

12-LO has also been implicated in normal function and pathologies of the mammalian eye. Thus, 12(*S*)-HETE has been suggested to promote PKC activation in lens epithelial cells, 12-LO is expressed in corneal epithelial cells, and 12(*R*)-HETE is a potent chemotactic and proangiogenic factor produced by the cornea (20, 21). Only very recently, expression of 12-LO was shown to be upregulated in oxygen-induced ischemic retinopathy and proliferative diabetic retinopathy suggesting its involvement in retinal neovascularization (22). Clearly, our results indicate that 12-LOs may play hitherto unrecognized roles in the development and function of the eye.

Zf12-LO Appears to Be Involved in Maintenance of the Permeability Barrier of the Embryo. Zf12-LO is expressed in epithelial cells of skin, stomodeum, pharyngeal pouches, and yolk sac (Fig. 2). Furthermore, transversal sections of the gut/kidney layer of MO treated embryos revealed deattachment of the epidermis from the yolk sac and the presence of a yolk sac edema indicating a role for zf12-LO in the maintenance of the permeability barrier of the embryo (Fig. 4). The cellular and extracellular fluids of freshwater fish like zf are hyperosmotic compared to the surrounding water. To stay in osmotic balance, these fishes have to maintain a barrier against water entry and excrete excess water that passes the barrier. For this homeostasis, the fish is dependent on gills, the skin, and kidney. The chorion is not essential for this process, as dechorionated embryos can exclude water without problems. The water permeability barrier on the surface of the developing embryo is composed of two separate barriers: one surrounding the embryo and another surrounding the yolk (23). The retention of water leading to pericardial and yolk sac edema, as observed in morphant embryos (Figs. 3, 4), may in principle be due to a barrier dysfunction or a kidney insufficiency. Because during the first two days of zf development the embryos do not possess a functional kidney (16), it is unlikely that the edemas are caused by an insufficient excretion of excess water. More likely, the observed edemas in MO treated embryos resulted from an imbalance in the permeability barrier of the skin.

Interestingly, studies of 12R-LO knock-out mice have indicated that this enzyme is involved in maintenance of the skin permeability barrier (14). In contrast, mice deficient in platelet 12S-LO exhibited only a minor enhancement of basal transepidermal water loss in the absence of apparent membrane ultra-

structural defects (24). Furthermore, for 12R-LO, molecular genetic studies have demonstrated that mutations within the gene coding for human 12R-LO give rise to a scaly skin phenotype known as autosomal recessive congenital ichthyosis (12). In the skin, 12R-LO is believed to function in tandem with an epidermal LO (eLOX3), which isomerizes 12(*R*)-hydroperoxy-fatty acids provided by 12R-LO into epoxy alcohols, termed hepoxilin A3 (25). Only recently, it was proposed that 12R-LO and eLOX3 act sequentially on *O*-linoleoyl-*ω*-hydroxy-ceramide to generate the 9(*R*)-hydroperoxy derivate of the esterified linoleate followed by isomerization into the corresponding epoxy alcohol, ketone, and epoxy-ketone derivatives (26). This regio- and stereospecific oxygenation of linoleate will facilitate ester hydrolysis, release of *ω*-hydroxy ceramide, and its subsequent binding to protein, which in turn is a molecular determinant for maintenance of the epidermal permeability barrier (26). Further work will tell whether zf12-LO, which is an LO with strict S-stereospecificity, carries out similar types of chemistry.

Zf12-LO Displays Features of Both S and R Mammalian 12-LOs. The number of 12-LO isoforms vary among species. Former studies discovered a 12-LO activity in several marine animals such as sea urchin, fish, or amphibians. In oocytes of sea urchin (*Strongylocentrotus purpuratus*), 12(*R*)-HETE production was demonstrated via stereospecific analysis (27). Investigations in rainbow trout displayed the presence of 12-LO(s) in blood cells (28) and gill tissue (29). The produced 12(*S*)-HETE together with PGE_2 seemed to play a role in the uptake of yeast particles through the macrophages of the fish (30). Additionally, in neurons of *Xenopus* 12-HETE production was verified (31). However, no investigations on the role of 12-LO(s) in the development of these organisms and the consequences of eliminating protein expression were done. Furthermore, it is discussed if a single ancient precursor of 12-LOs exists and, if so, when the division into different 12-LO subtypes occurred in evolution (2, 32).

Zf12-LO was the only 12-LO orthologue found upon screening the zf whole genome shotgun assembly Zv7. The zf12-LO primary structure carries several motifs that are found among 12S-LOs (Figs. S1, S2). However, the protein also contains a Gly residue at the Coffa site, typical of R-specific LOs but displays a strict S-stereospecificity (Fig. 1). Moreover, upon knock-down of the zf12-LO protein, a dramatic phenotype is generated suggesting its involvement in *inter alia* regulation of the epidermal permeability barrier, a function previously described for mammalian 12R-LO (14). Hence, it seems that zf12-LO, a vertebrate LO, merges structural, catalytic, and functional characteristics of both 12S- and 12R-LO into a single protein and may therefore give clues to the evolutionary development that led to the multiple 12-LO isoforms found in mammals.

Experimental Procedures

Determination of zf12-LO Enzyme Activity by LC-MS. Recombinant zf12-LO protein (for cloning, expression, and purification, see *SI Materials and Methods*) was incubated with substrate mix (100 μM arachidonic acid, 12.5 mM ATP) in A-buffer (50 mM Tris/HCl, pH 7.5, 10 mM EDTA, 2.2 mM $CaCl_2$, 2 mM DTT) for 30 min at 37 °C. The reaction was stopped by adding 3 volumes of acetonitrile/H_2O/acetic acid, 60:40:0.1, (vol/vol) and loaded on a C18-column (SUPELCO). Compounds were eluted with 100% methanol. Hydroperoxy-fatty acids were reduced into hydroxy-fatty acids with $NaBH_4$ (10 μg/μL, 30 min at room temperature) and loaded on a second C18-column. Metabolites were eluted with 100% methanol and analyzed via LC-MS. A Thermo Finnigan Surveyor System, with a quaternary pump, in-line degasser, and a thermostated autosampler, equipped with a 2.0 × 150 mm, 5 μm Luna C18 column (Phenomenex) was used. The gradient was generated with four solvents: A (H_2O), B (acetonitrile/MeOH, 88:12), C (H_2O/0.1% acetic acid), and D (acetonitrile/MeOH/acetic acid, 88:12:0.1) at a flow rate of 350 μL/min. The gradient started with 85% A and 15% B for 0.5 min. The solvent B is then increased to 30% from 0.5 to 2 min, to 55% from 2 to 8 min, to 75% from 8 to 28 min, and finally to 100% from 28 to 28.5 min. The effluent was connected to an ion trap mass spectrometer (LCQ Deca, Finnigan MAT) and subjected to electrospray ionization. The capillary temperature was set at 250 °C, and the shealth and auxiliary gas flow rates were set to 70 and 20 arbitrary units, respectively. All spectra were collected in negative ion mode and single reaction monitoring mode. The collision energy was set to 40%. The transition ions monitored were 319.2 to: 5-HETE = 115; 8-HETE = 155; 9-HETE = 123; 11-HETE = 167; 12-HETE = 179; 15-HETE = 219; 16-HETE = 121; and 20-HETE = 275. All spectra were processed using the Qual Browser program present in the Xcalibur program version 2.0.

Assessment of the Stereospecificity of zf12-LO. Recombinant zf12-LO was incubated with arachidonic acid as described above. The metabolites were reduced using $NaBH_4$, extracted on a C18-column (SUPELCO), methyl-esterified by treatment with diazomethane and analyzed by CP-HPLC using an OB-H column (250 × 4.6 mm; Daicel Chemical Industries). Elution was accomplished with 2-propanol-hexane (2:98, vol/vol) at a flow rate of 0.5 mL/min, and the absorbance at 234 nm was used for detection of enantiomers of 12-HETE methyl esters.

Zebrafish Strain and Maintenance. Adult fishes of the AB strain were maintained and mated accordingly to standard procedures (33). Embryos were kept in 0.003% 1-phenyl-2-thiourea treated egg-water and staged according to hours/days post fertilization and morphological features (16). When necessary, the embryos were anaesthetized using 4 mg/mL Tricaine (Sigma).

Immunohistochemistry. Zf embryos were embedded in O.C.T.™ Compound (Tissue-Tek, HistoLab), slowly frozen on dry ice and cut into 10 μm sections. Sections were fixed in ethanol in −20 °C for 20 min, blocked at room temperature for 2 h in TNB blocking buffer (TSA Biotin System, Perkin Elmer Life Science) supplemented with 10% normal goat serum and 4% BSA, and then incubated with IgG purified antibody against zf12-LO (diluted 1:50) at 4 °C over night. For details of the rabbit polyclonal antibody, see *SI Materials and Methods*. After several washes in Tris-NaCl-Tween washing buffer (TSA Biotin System, Perkin Elmer Life Science), sections were incubated with secondary Alexa Fluor 488 goat anti-rabbit IgG (1:1,000, Molecular Probes) at room temperature for 1 h. After washing, nuclei were counterstained using DAPI and the sections were mounted and examined using a Zeiss Axiophot fluorescence microscope.

Antisense Morpholino Oligonucleotide Design and Embryo Microinjections. Antisense MOs were designed according to the guidelines of Gene Tools, LLC using the sequence from *zf* AB genomic DNA. A translation-blocking MO sequence (MO-1) against the start site of *zfalox12* (5′-GTACTCCATCTGCACACATACACGT-3′) as well as a splice-blocking (exon2-intron2) MO (MO-2) (5′-CAATCAATGTAACTGACCTGTGCCT-3′) was used. As control the following corresponding 5-mispair (mis) MOs were used. MO-1 mis: 5′-GTA**g**TC**g**ATCT**c**CACA**g**ATA**g**ACGT-3′; MO-2 mis: 5′-CAATCAAT**c**TAA**g**TGA**a**CT**c**TG**g**CT-3′. Prior to injection MOs were diluted in 0.2 mM KCl supplemented with 1% rhodamine conjugated 70 kDa-dextran (Invitrogen). To avoid potential toxicity of MOs and obtain viable embryos with consistent phenotypes, the amount of MO used to inject embryos was titrated out (125–500 μM). Finally, MO solutions were injected into embryos at the one- to two-cell stage with a final concentration of 250 μM MO-1/MO-1 mis and 500 μM MO-2/MO-2 mis (10 nL/embryo). Morphants were analyzed from multiple injected clutches. For macroscopic phenotypic analyses, pictures of

three different groups of embryos (normal, moderate, and severe phenotype) were taken. For microscopic analyses of the organs embryos were embedded in plastic, for details see *SI Materials and Methods*.

1. Brash AR (1999) Lipoxygenases: occurrence, functions, catalysis, and acquisition of substrate. *J Biol Chem* 274:23679–23682.
2. Kuhn H, O'Donnell VB (2006) Inflammation and immune regulation by 12/15-lipoxygenases. *Prog Lipid Res* 45:334–356.
3. Samuelsson B (1983) Leukotrienes: mediators of immediate hypersensitivity reactions and inflammation. *Science* 220:568–575.
4. Serhan CN, Chiang N, Van Dyke TE (2008) Resolving inflammation: dual anti-inflammatory and pro-resolution lipid mediators. *Nat Rev Immunol* 8:349–361.
5. Haeggström JZ, Funk CD (2011) Lipoxygenase and leukotriene pathways, biochemistry, biology and roles in disease. *Chem Rev* 111:5866–5898.
6. Schneider C, Pratt DA, Porter NA, Brash AR (2007) Control of oxygenation in lipoxygenase and cyclooxygenase catalysis. *Chem Biol* 14:473–488.
7. Coffa G, Brash AR (2004) A single active site residue directs oxygenation stereospecificity in lipoxygenases: stereocontrol is linked to the position of oxygenation. *Proc Natl Acad Sci USA* 101:15579–15584.
8. Boeglin WE, Kim RB, Brash AR (1998) A 12R-lipoxygenase in human skin: mechanistic evidence, molecular cloning, and expression. *Proc Natl Acad Sci USA* 95:6744–6749.
9. Sun D, et al. (1998) Human 12(R)-lipoxygenase and the mouse ortholog. Molecular cloning, expression, and gene chromosomal assignment. *J Biol Chem* 273:33540–33547.
10. Pidgeon GP, et al. (2007) Lipoxygenase metabolism: roles in tumor progression and survival. *Cancer Metastasis Rev* 26:503–524.
11. Wang D, Dubois RN (2010) Eicosanoids and cancer. *Nat Rev Cancer* 10:181–193.
12. Jobard F, et al. (2002) Lipoxygenase-3 (ALOXE3) and 12(R)-lipoxygenase (ALOX12B) are mutated in non-bullous congenital ichthyosiform erythroderma (NCIE) linked to chromosome 17p13. *Hum Mol Genet* 11:107–113.
13. Johnson EN, Brass LF, Funk CD (1998) Increased platelet sensitivity to ADP in mice lacking platelet-type 12-lipoxygenase. *Proc Natl Acad Sci USA* 95:3100–3105.
14. Epp N, et al. (2007) 12R-lipoxygenase deficiency disrupts epidermal barrier function. *J Cell Biol* 177:173–182.
15. Grunwald DJ, Eisen JS (2002) Headwaters of the zebrafish—emergence of a new model vertebrate. *Nat Rev Genet* 3:717–724.
16. Kimmel CB, Ballard WW, Kimmel SR, Ullmann B, Schilling TF (1995) Stages of embryonic development of the zebrafish. *Dev Dyn* 203:253–310.
17. Sloane DL, Leung R, Craik CS, Sigal E (1991) A primary determinant for lipoxygenase positional specificity. *Nature* 354:149–152.
18. Bendani MK, et al. (1995) Localization of 12-lipoxygenase mRNA in cultured oligodendrocytes and astrocytes by in situ reverse transcriptase and polymerase chain reaction. *Neurosci Lett* 189:159–162.

ACKNOWLEDGMENTS. The authors thank Eva Ohlson and Anders Wetterholm for technical assistance. The work was financed by the Swedish Research Council, European Union (201668), Vinnova (Chronic Inflammation, Diagnosis, and Therapy), Torsten & Ragnar Söderbergs Foundation and a Distinguished Professor Award (J.Z.H.) from Karolinska Institutet.

19. Phillis JW, Horrocks LA, Farooqui AA (2006) Cyclooxygenases, lipoxygenases, and epoxygenases in CNS: their role and involvement in neurological disorders. *Brain Res Rev* 52:201–243.
20. Liminga M, Oliw EH (2000) Studies of lipoxygenases in the epithelium of cultured bovine cornea using an air interface model. *Exp Eye Res* 71:57–67.
21. Masferrer JL, et al. (1991) 12(R)-hydroxyeicosatrienoic acid, a potent chemotactic and angiogenic factor produced by the cornea. *Exp Eye Res* 52:417–424.
22. Al-Shabrawey M, et al. (2011) Increased expression and activity of 12-lipoxygenase in oxygen-induced ischemic retinopathy and proliferative diabetic retinopathy: implications in retinal neovascularization. *Diabetes* 60:614–624.
23. Hagedorn M, Kleinhans FW, Artemov D, Pilatus U (1998) Characterization of a major permeability barrier in the zebrafish embryo. *Biol Reprod* 59:1240–1250.
24. Johnson EN, Nanney LB, Virmani J, Lawson JA, Funk CD (1999) Basal transepidermal water loss is increased in platelet-type 12-lipoxygenase deficient mice. *J Invest Dermatol* 112:861–865.
25. Yu Z, Schneider C, Boeglin WE, Marnett LJ, Brash AR (2003) The lipoxygenase gene ALOXE3 implicated in skin differentiation encodes a hydroperoxide isomerase. *Proc Natl Acad Sci USA* 100:9162–9167.
26. Zheng Y, et al. (2011) Lipoxygenases mediate the effect of essential fatty acid in skin barrier formation: A proposed role in releasing omega-hydroxyceramide for construction of the corneocyte lipid envelope. *J Biol Chem* 286:24046–24056.
27. Hawkins DJ, Brash AR (1987) Eggs of the sea urchin, Strongylocentrotus purpuratus, contain a prominent (11R) and (12R) lipoxygenase activity. *J Biol Chem* 262:7629–7634.
28. Hill DJ, Griffiths DH, Rowley AF (1999) Trout thrombocytes contain 12- but not 5-lipoxygenase activity. *Biochim Biophys Acta* 1437:63–70.
29. German JB, Bruckner GG, Kinsella JE (1986) Lipoxygenase in trout gill tissue acting on arachidonic, eicosapentaenoic and docosahexaenoic acids. *Biochim Biophys Acta* 875:12–20.
30. Knight J, Lloyd-Evans P, Rowley AF, Barrow SE (1993) Effect of lipoxins and other eicosanoids on phagocytosis and intracellular calcium mobilisation in rainbow trout (Oncorhynchus mykiss) leukocytes. *J Leukocyte Biol* 54:518–522.
31. Nishiyama M, et al. (2003) Cyclic AMP/GMP-dependent modulation of Ca^{2+} channels sets the polarity of nerve growth-cone turning. *Nature* 423:990–995.
32. Toh H, Yokoyama C, Tanabe T, Yoshimoto T, Yamamoto S (1992) Molecular evolution of cyclooxygenase and lipoxygenase. *Prostaglandins* 44:291–315.
33. Brand M, Granato M, Nüsslein-Volhard C (2002) *Zebrafish*, eds C Nüsslein-Volhard and R Dahm (Oxford University Press, New York), pp 7–37.